Morphological Characterization of Bicontinuous Phase-Separated Polymer Blends and One-Phase Microemulsions

Hiroshi Jinnai,*,† Takeji Hashimoto,*,†,‡ Daniel Lee,§ and Sow-Hsin Chen⊥

Hashimoto Polymer Phasing Project, ERATO, Japan Science and Technology Corporation, Keihan-na Plaza, 1-7 Hikari-dai, Seika, Kyoto 619-02, Japan, Department of Polymer Chemistry, Graduate School of Engineering, Kyoto University, Kyoto 606, Japan, and Departments of Physics and Nuclear Engineering, Massachusetts Institute of Technology, Cambridge, Massachusetts 02139

Received April 1, 1996; Revised Manuscript Received September 25, 1996⊗

ABSTRACT: The morphological similarity between a phase-separated polymer blend and a one-phase bicontinuous microemulsion is discussed in detail by comparing their respective light and X-ray scattering intensity distributions with structure factors computed according to the random wave model (RWM). In the RWM, a three-parameter spectral function introduced by Lee and Chen is used in conjunction with Berk's theory and Cahn's clipping scheme to calculate the Debye correlation function for the scattering intensity. The agreement between experiment and theory is excellent. The three parameters determined by fitting the scattering intensities are then used to calculate the average Gaussian curvature of the interfaces between the two isometric phases for the first time. The RWM can also be used to generate the 3D morphologies of both the bicontinuous phase-separated polymer blend and the one-phase microemulsion. There is a striking resemblance between the morphologies of these two unrelated systems, in spite of a difference in length scales characterizing the structures of a factor of about 250.

Introduction

Studies of bicontinuous and interpenetrating domain structures developed via spinodal decomposition (SD) have been an attractive research theme among researchers dealing with binary mixtures of molecular fluids, binary alloys, and polymer blends over the past decades.[1,2] Complex structures can be observed in the phase separation process induced by a temperature quench from the stable one-phase region into the unstable two-phase spinodal region. The fact that the dynamical processes in complex fluids such as polymer blends, glasses, and gels are extremely slow due to their long characteristic relaxation times allows us to study their morphologies with better accuracy than those of simple liquid mixtures.[3]

Similar kinds of bicontinuous structures have been observed in a water/oil/surfactant three-component microemulsion system in the one-phase region close to the three-phase boundary and in the vicinity of the hydrophile−lipophile balance temperature.[4] It is interesting to examine the common and universal features, if they exist, of the bicontinuous structures observed in phase-separated polymer blends and in microemulsions.

Scattering techniques such as light (LS), small-angle X-ray (SAXS), and small-angle neutron (SANS) have been extensively used to examine the structure factors of the phase-separated structures of polymer blends.[2,5,6] Structure factors, which describe the scattering length density distribution of the phase-separated structure, have been compared with theories[7] and with the results of computer simulations.[8] The structure factor of phase-separated polymer blends has a maximum intensity at $q = q_m$ (q is the magnitude of the scattering vector) and a weak shoulder-like secondary maximum around $q \cong 3q_m$, which is well described by computer simulations based on a numerical solution of the time-dependent Ginzburg−Landau (TDGL) equation.[8] An approximate theory by Ohta and Nozaki[9] based on the interfacial equation of motion is also successful in describing such a structure factor.

In bicontinuous microemulsions, a theory developed by Berk[10] has been used to analyze scattering data and to generate the three-dimensional (3D) morphology corresponding to the scattering data. A random Gaussian field that is generated by superposing many isotropically propagating sinusoidal waves with random phases is "clipped" to simulate the two-phase morphology whose essential features depend on the spectral function. It should be noted that this idea was first developed by Cahn[11] for generating the 3D morphology formed by SD. Chen et al. proposed a peaked spectral function with a power law decay at large wave numbers which was able to reproduce their SANS intensity distributions from the microemulsions (called a modified Berk, or MB, theory).[12] Moreover, Chen et al. used the MB theory to estimate the average Gaussian curvature, $\langle K \rangle$, of their microphase-separated bicontinuous structure.[13]

In the present paper, we apply the MB theory to the scattering data from a polymer blend (which is in a nonequilibrium state) in order to see whether or not there are some common features shared by these two dynamically disparate systems. It is worth noting that the two systems have *very* different characteristic lengths: the characteristic length of the phase-separated polymer blend used here is of the order of 10 μm, while that of the microemulsion is of the order of 100 Å. We use Berk's theory to construct 3D images for both the polymer blend and the microemulsion. A *real* 3D picture observed by laser scanning confocal microscopy (LSCM) is then presented for comparison.

Experimental Section

The polymer blend used in the present study was a near-critical mixture of perdeuterated polybutadiene (dPB) and polyisoprene (PI). Both polymers were synthesized by living anionic polymerization. The number-average molecular weight

† Japan Science and Technology Corp.
‡ Kyoto University.
§ Department of Physics, MIT.
⊥ Department of Nuclear Engineering, MIT.
⊗ Abstract published in *Advance ACS Abstracts,* December 15, 1996.

S0024-9297(96)00486-X CCC: $14.00

(M_n) of dPB was 6.1×10^4, with a molecular weight distribution, characterized by M_w/M_n (M_w is weight-averaged molecular weight) of 1.07. PI had $M_n = 1.41 \times 10^5$ and $M_w/M_n = 1.04$. dPB/PI blend mixtures with a composition of 39 wt % dPB and 61 wt % PI were dissolved in toluene and subsequently cast to form films. SANS experiments were made on the dPB/PI blend, from which it was shown that the mixture was characterized by a lower critical solution temperature (LCST)-type phase diagram with a spinodal temperature of 36 ± 1 °C at the composition studied here. A temperature jump from 25 to 70 °C was used to induce phase separation via SD. The phase separation process was followed by a time-resolved light scattering (LS) experiment that gave the scattering intensity, $I(q,t)$, as a function of wave number q at time t. q is defined by

$$q = \frac{4\pi n}{\lambda_0} \sin\left(\frac{\theta}{2}\right) \tag{1}$$

where λ_0 and θ are, respectively, wavelength of light in the vacuum ($\lambda_0 = 632.8$ nm) and scattering angle in the medium. n is the average refractive index of the mixture.

For the microemulsion, ternary mixtures of heavy water (D_2O), *n*-octane, and tetraethylene glycol monodecyl ether (C_4E_{10}) were used. Volume fractions of the surfactant (ϕ_s), water (ϕ_w), and oil (ϕ_0) were respectively 0.130, 0.435, and 0.435. For a nonionic surfactant of this type, at low temperatures the hydrophilicity of the surfactant dominates, resulting in a two-phase equilibrium between a relatively pure oil phase on the top and a water phase containing most of the surfactant forming an oil-in-water microemulsion in the bottom. On the other hand, at high temperatures, because the formation of hydrogen bonds becomes thermodynamically less favorable, the surfactant becomes less hydrophilic and tends to go to the oil-rich phase on the top, forming a water-in-oil microemulsion. Between these two extremes, there is a range of temperatures where the hydrophobic nature of the hydrocarbon tail of the surfactant is nearly matched by the hydrophilicity of the molecular head group. At such temperatures, the one-phase microemulsion becomes thermodynamically stable. For the particular concentration of surfactant used here, the one-phase region spans the temperature range from about 19 to 25 °C. We note here that the term "one-phase" microemulsion does not necessarily imply that the three components are miscible at the molecular level. Observationally, it only means that the system is not macroscopically phase-separated. In the one-phase microemulsion, at moderate surfactant concentration, it is known that a microphase-separated structure exists in *thermal equilibrium*. The microstructure consists of interpenetrating domains of water and oil, having characteristic dimensions of the order of 100 Å, with most of the surfactant molecules sitting at the interface.

SAXS measurements were made for the microemulsion using an apparatus having a 18 kW rotating-anode X-ray generator (MAC Science Co Ltd., Yokohama, Japan) as a source. A graphite crystal was used to select the Cu Kα line with the characteristic wavelength $\lambda = 1.542$ Å. Sample-to-detector distance was 1988 mm, and a one-dimensional position-sensitive proportional counter was used as a detector. SAXS profiles were corrected for absorption, air scattering, sample thickness, slit height and slit width smearing, and the thermal diffuse scattering arising from density fluctuations.

Theoretical Background

In general, the intensity distribution of LS and SAXS from an isotropic two-component porous material can be calculated from a Debye correlation function, $\Gamma(r)$, by using the following formula:[14]

$$I(q) = \langle \eta^2 \rangle \int_0^\infty \mathrm{d}r\, 4\pi\, r^2\, j_0(qr)\Gamma(r) \tag{2}$$

where $\langle \eta^2 \rangle = \nu_A \nu_B (\rho_A - \rho_B)^2$. ν_A and ν_B refer to the volume fractions of the phases rich in A and B and ρ_A and ρ_B to the corresponding scattering length densities. Besides the two physical boundary conditions that the Debye correlation function is normalized to unity at the origin and should go to zero at infinity, the most important property of the correlation function is that it has a linear term in the small r expansion to ensure a finite interfacial area per unit volume, S/V, of the form

$$\Gamma(r \to 0) = 1 - \frac{1}{4\nu_A\nu_B}\frac{S}{V} r + \cdots \tag{3}$$

In 1965, Cahn proposed[11] a scheme for generating a 3D morphology of a phase-separated A−B alloy by clipping a Gaussian random field generated by superposing many isotropically propagating sinusoidal waves with random phases. In 1987, Berk further extended the idea of Cahn for the purpose of analyzing scattering data.[10] In particular, he derived an important relation connecting the two-point correlation function of the underlying Gaussian random field and the Debye correlation function, describing the positional correlation of the scattering length density, required to calculate the scattering intensity. In his original paper, however, Berk discussed only a spectral function which is a delta function. This produced a morphology that is only partially disordered.

In the random wave model of Berk, the Gaussian random field, $\Psi(\vec{r})$, is constructed by the following sum:

$$\Psi(\vec{r}) = \frac{1}{\sqrt{N}} \sum_{i=1}^{N} \cos(\vec{k}_i \cdot \vec{r} + \varphi_i) \tag{4}$$

where the directions of the wave vector $\vec{k}_i$ are sampled isotropically over a unit sphere and the phase φ_i is distributed randomly over the interval $(0,2\pi)$. Note that the Gaussian random field is normalized so that the field describing the local composition of A and B fluctuates continuously between −1 and 1 as $N \to \infty$. The statistical properties of the Gaussian random process are completely characterized by giving its two-point correlation function $g(|\vec{r}_1 - \vec{r}_2|) = \langle \Psi(\vec{r}_1)\Psi(\vec{r}_2) \rangle$ and the associated spectral function $f(k)$, which is related by a Fourier transform relation:

$$g(|\vec{r}_1 - \vec{r}_2|) = \int_0^\infty 4\pi k^2 j_0(k|\vec{r}_1 - \vec{r}_2|) f(k)\, \mathrm{d}k \tag{5}$$

We note that $f(k)$ gives the distribution of the magnitudes of the propagating wave vectors of the sinusoidal waves and describes the essential features of the morphology. From eq 5, one has a small r expansion of $g(r)$ of the form

$$\begin{aligned} g(r) &= \int_0^\infty 4\pi k^2 \left[1 - \frac{1}{6}k^2 r^2 + \cdots\right] f(k)\, \mathrm{d}k \\ &= 1 - \frac{1}{6}\langle k^2 \rangle r^2 + \cdots \end{aligned} \tag{6}$$

where we used the normalization condition $g(0) = 1$. Note that this expansion has a quadratic dependence on r in the second term.

This continuous Gaussian random process is then clipped and transformed into a two-state discrete random process. Namely, the process assigns −1 to all negative signals representing A and +1 to all positive signals representing B. Then, the Debye correlation function for this discrete random process for the isometric case, namely $\nu_A = \nu_B$, is given exactly as[10]

$$\Gamma(r) = \frac{2}{\pi} \sin^{-1}(g(r)) \tag{7}$$

Using the result of eq 6 in eq 7, we obtain the correct expansion for the Debye correlation function (cf. eq 3):

$$\Gamma(r \to 0) = 1 - \frac{2}{\pi\sqrt{3}}(\langle k^2 \rangle)^{1/2}\, r + \cdots \tag{8}$$

We next consider a random surface generated by the level set

$$\psi(\vec{r}) = \psi(x,y,z) = 0 \tag{9}$$

Teubner[15] has proved the remarkable theorem that, for this random surface, the mean curvature is zero and the Gaussian curvature $\langle K \rangle$ is negative and given by

$$\langle K \rangle = -\frac{1}{6}\langle k^2 \rangle \tag{10}$$

Since the level surface defined by eq 9 corresponds either to the interface between the two coexisting phases for the polymer blend or to the midplane of the surfactant monolayer for an isometric, bicontinuous microemulsion, $\langle K \rangle$ of the interface (or surfactant monolayer) can be computed once $f(k)$ is found.

A suitable form of the spectral function was proposed by Lee and Chen,[12] which is an inverse sixth-order polynomial in k containing three parameters, a, b, and c:

$$f(k) = \frac{8\pi b[a^2 + (b+c)^2]/(2\pi)^3}{(k^2 + c^2)[k^4 - 2(a^2 - b^2)k^2 + (a^2 + b^2)^2]} \tag{11}$$

This form is an extension of the well-known structure factor, proposed by Teubner and Strey[16] for the bicontinuous microemulsion, in such a way that it possesses a definite second moment. The corresponding two-point correlation function can also be written down analytically using eq 5 and has a quadratic term in the small r expansion:

$$\begin{aligned} g(r) &= \frac{1}{a^2 + (c^2 - b^2)}\left\{(a^2 + c^2 - b^2)\frac{\sin(ar)}{ar}\, e^{-br} + 2b\frac{e^{-cr} - e^{br}\cos(ar)}{r}\right\} \\ &= 1 - \frac{1}{6}\left\{\frac{(a^2 + b^2)^2 + c^2(a-b)(a+3b)}{a^2 + (c-b)^2}\right\} r^2 + \cdots \\ &= 1 - \frac{1}{6}\langle k^2 \rangle r^2 + \cdots = 1 + \langle K \rangle r^2 + \cdots \end{aligned} \tag{12}$$

The intensity distribution of LS and SAXS can be calculated by using this $g(r)$ substituted into eqs 2, 5, and 7, which is used to fit the scattering data to evaluate the three parameters, a, b, and c. The first two parameters, a and b, have their approximate correspondence in the Teubner−Strey (TS) theory.[17] In the TS theory, the Debye correlation function is given by $\Psi_{TS}(r) = e^{-r/\xi}[\sin(2\pi r/d)/(2\pi r/d)]$. The correspondences are $a \approx 2\pi/d$ and $b \approx 1/\xi$, where d is the interdomain repeat distance and ξ the coherence length of the local order.[17] The parameter c controls the large q behavior of the scattering intensity of the MB theory, and experiments at large q as will be seen later. $1/c$ may be related to the persistence length of the interface.[12]

Now, from eq 12, the average Gaussian curvature is given by

$$\langle K \rangle = -\frac{1}{6}\left\{\frac{(a^2 + b^2)^2 + c^2(a-b)(a+3b)}{a^2 + (c-b)^2}\right\} \tag{13}$$

Results and Discussion

By assuming an existence of a characteristic length scale Λ for the microstructure of a two-phase medium, we can write the Debye correlation function in the scaling form $\Gamma(r/\Lambda)$.[18] Equation 2 for the scattering intensity can then be transformed into the form

$$I(q) \sim \langle \eta^2 \rangle \Lambda^3 S(q\Lambda) \tag{14}$$

where $\langle \eta^2 \rangle$ is the mean-square fluctuation of the scattering length density.[19] The scattering length density contrast arises from the refractive index difference between dPB and PI for the case of LS and the electron density difference between heavy water and *n*-octane for the case of SAXS, respectively. $S(q\Lambda)$ is a dimensionless function called the "scaled structure factor", which characterizes isotropically and orientationally the averaged q-space structure of the system. $I(q)$ from the dPB/PI mixture undergoing SD shows a maximum intensity at $q = q_m$ which is proportional to the inverse to the characteristic length of the system, i.e., $\Lambda \sim q_m^{-1}$. Hence, eq 14 can be rewritten as

$$\frac{q_m{}^3 I(q)}{\langle \eta^2 \rangle} \sim S(q\Lambda) \tag{15}$$

Here, $\langle \eta^2 \rangle$ can be experimentally obtained from the following integral:

$$\langle \eta^2 \rangle \sim \int_0^\infty I(q) q^2\, dq \tag{16}$$

Figure 1 shows a log−log plot of $q_m{}^3 I(q)/\langle \eta^2 \rangle$ as a function of the reduced wavenumber q/q_m ($\sim q\Lambda$) both for the dPB/PI blend at $t = 114.6$ min and for the microemulsion at various temperatures. We note that the profile of dPB/PI was taken in the late stage of SD ($\tau \approx 288$, where τ is a reduced time defined by $\tau = t/t_c$, where t_c is a characteristic time of the system).[20]

The overall shape of $S(q\Lambda)$ was similar between the two systems, suggesting that, in a statistical sense, the characteristic features of the two morphologies are similar. Both systems showed a peaked scattering profile and have asymptotic q^{-4} behaviors for sufficiently large q. This is the Porod asymptotic scattering[21] law for a sharp interface. For the dPB/PI blend, $S(q\Lambda)$ had q^{-n} ($n > 6$) behavior for $1 \le q/q_m \le 2$ and q^{-4} behavior for $q/q_m \ge 3$. We note that there is a small high-order shoulder at $q/q_m \approx 3$ for the dPB/PI blend. The same trend was observed for the microemulsion, except for the fact that the Porod law region is a bit narrower, i.e., $1.5 \le q/q_m \le 3$, compared to that of the polymer blend. The crossover from q^{-n} to q^{-4} was less distinct for the microemulsion.

In the q range where $q/q_m < 1$, the slopes of $S(q\Lambda)$ were significantly different. The dPB/PI mixture had a slope of about 4, which appeared to be consistent with the theory of Furukawa[22] and that of Yeung[23] for a spinodally decomposed bicontinuous structure. In contrast, in the same q range, the microemulsion had a shallower slope (about 2 or less) than the dPB/PI did.

For the microemulsion, $S(q\Lambda)$ at different temperatures fell nicely onto a single curve in $q/q_m > 1$, although

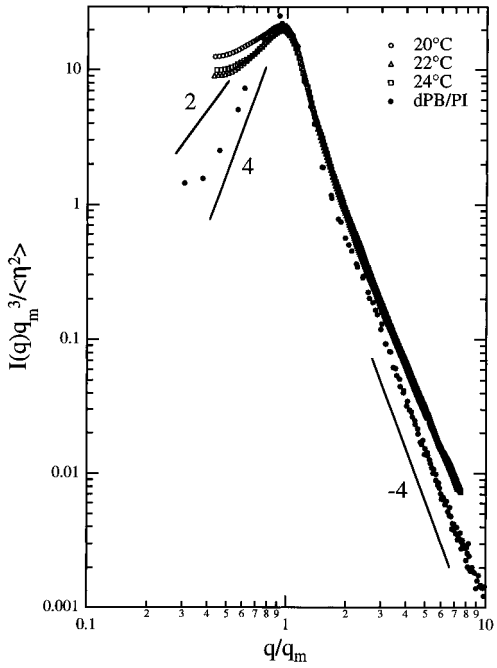

Figure 1. Scaled scattering intensity as a function of scaled scattering vector for the dPB/PI blend and for the microemulsion at different temperatures: 20, 22, and 24 °C. Solid lines represent power law behavior of the scaled scattering intensities whose exponents are specified by numbers.

it showed some temperature dependence for $q/q_m < 1$. Detailed analysis of the SAXS data is presented elsewhere.[13]

Figure 2 shows the best fits of the MB theory (solid line) for both the microemulsion at 22 °C (part a) and the dPB/PI mixture (part b) in log−log plots. The dashed line in the figure represents the best fit obtained from the TS theory. Fitting the theories to SANS profiles of the microemulsion has already been discussed,[13] in which the MB theory described the scattering profiles more accurately, especially in the high q region, than the TS theory. This is also the case for the present SAXS study of the microemulsion. An excellent agreement between the SAXS profiles and the MB theory was obtained over the entire temperature range of our experiment. The theory fit over the whole q range except for the tails of the profiles, i.e., $q > 0.08$ Å^{-1}.

It is quite impressive that the MB theory also reproduced the LS profile (part b) for the dPB/PI blend, especially in the high q range including the shoulder. It is also worth noting that the TS theory failed to describe $I(q)$ in the large q region for the dPB/PI mixture. However, the fit was not as good in the low q range, i.e., $q < 9 \times 10^{-1}$ μm^{-1}. Both the TS and the MB theories showed shallower slopes in this q range than the experimental data. Furukawa predicted $I(q) \sim q^2$ behavior in $q/q_m < 1$, if thermal fluctuations are significant.[24] Hence, the discrepancy of the slope in $q/q_m < 1$ between the theories and the LS data may be due to the small effect on the thermal fluctuations to the large-scale morphology ($d \approx 7.1$ μm). On the other hand, sizes of phase-separated domains of the microemulsion are much smaller ($d \approx 303$ Å), and interfacial tension is lower, due to the existence of a surfactant film in the oil−water interface. In the latter case, the thermal noise is expected to have a larger effect on the microstructure, which leads to the weaker q dependence, i.e., $I(q) \sim q^2$. In any event, the fact that the same theory (MB theory) can reasonably describe scattering behaviors of two systems having very different characteristic lengths is remarkable. We therefore conclude that the morphologies of the phase-separated polymer blend and the microemulsions are quite similar, except for their length scales.

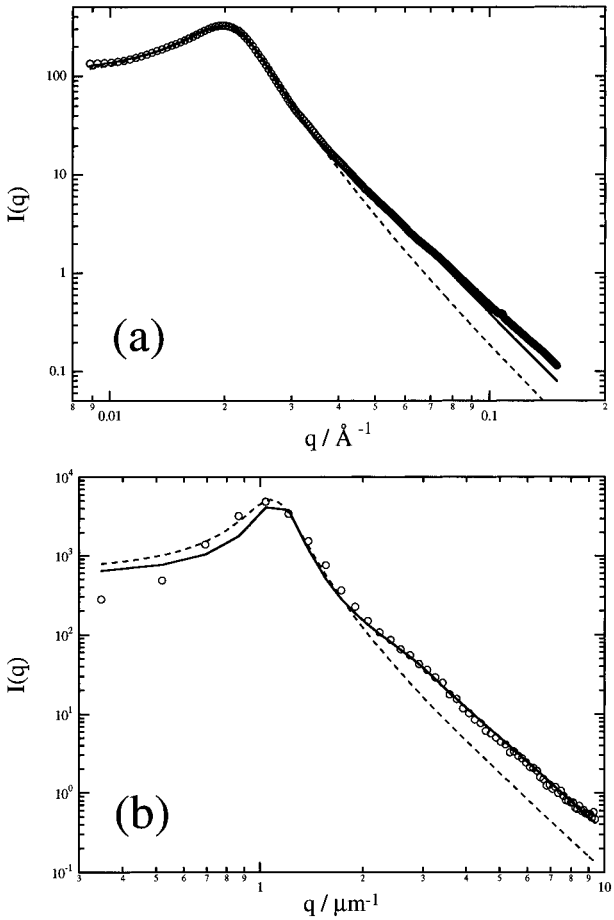

Figure 2. (a) Modified Berk model analysis of scattering intensity of the one-phase microemulsion. (b) Modified Berk model analysis of scattering intensity of the dPB/PI blend. Solid and dashed lines show the best fit using the MB theory and the TS theory, respectively.

Parameters used to obtain those fits, i.e., solid lines in Figure 2, were $a = 0.921$ μm^{-1}, $b = 0.147$ μm^{-1}, $c = 1.97$ μm^{-1} for the dPB/PI blend and $a = 2.07 \times 10^{-2}$ Å^{-1}, $b = 5.26 \times 10^{-3}$ Å^{-1}, $c = 4.53 \times 10^{-2}$ Å^{-1} for the microemulsion, respectively. As mentioned in the theory section, parameters a and b are proportional to d and ξ, respectively. We now define a disorder parameter, b/a, which is $(1/2\pi)(d/\xi)$: if the ratio is large, the coherence length of local order (ξ) is short compared to the periodicity of the order (d). The disorder parameters were 0.16 and 0.25 for dPB/PI blend and the microemulsion, respectively. We note here that $d/\xi = 0.16 \times (2\pi) \cong 1$ for the dPB/PI mixture, implying that the phase-separated structure of the polymer mixture can be characterized effectively by a single length scale. Furthermore, the parameter c is very close to 2 times the parameter a. On the other hand, d/ξ for the microemulsion is roughly 1.6, indicating that the structure is more disordered than the polymer mixture, probably because of the larger effect of thermal fluctuations, arising from the low interfacial tension, on the microstructure.

One of the advantages of using the MB theory is the fact that one can easily generate a 3D morphology which

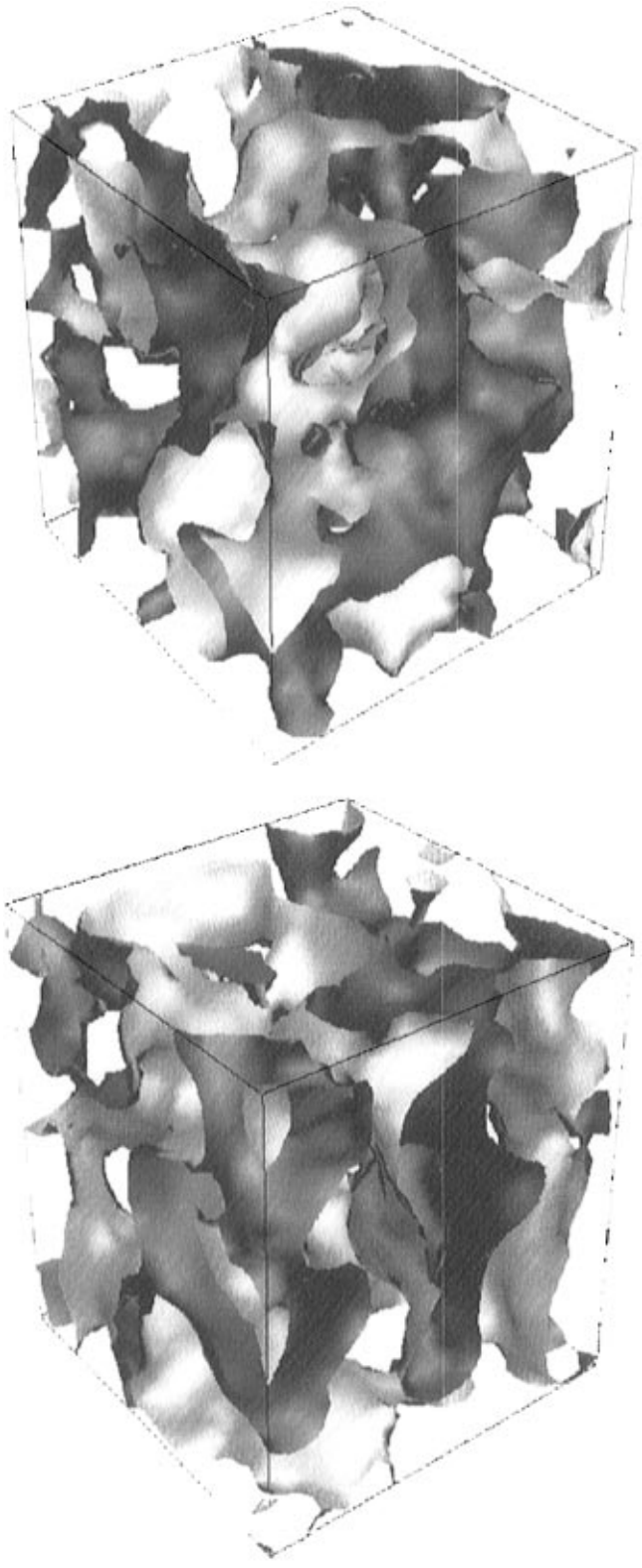

Figure 3. (a, top) 3D morphology of the phase-separated polymer blend (box size, $22.4^3\ \mu m^3$). (b, bottom) 3D morphology of the one-phase bicontinuous microemulsion at hydrophile–lipophile balanced temperature (box size, 800^3 Å^3). Both are generated from the MB theory with three fitting parameters obtained from the best fit to the corresponding scattering profiles.

is consistent with a scattering intensity distribution.[10] Figure 3 shows 3D morphologies on the basis of MB theory for the polymer blend (part a) and for the microemulsion (part b). In the figure, the interface between the two coexisting phases, i.e., dPB-rich and

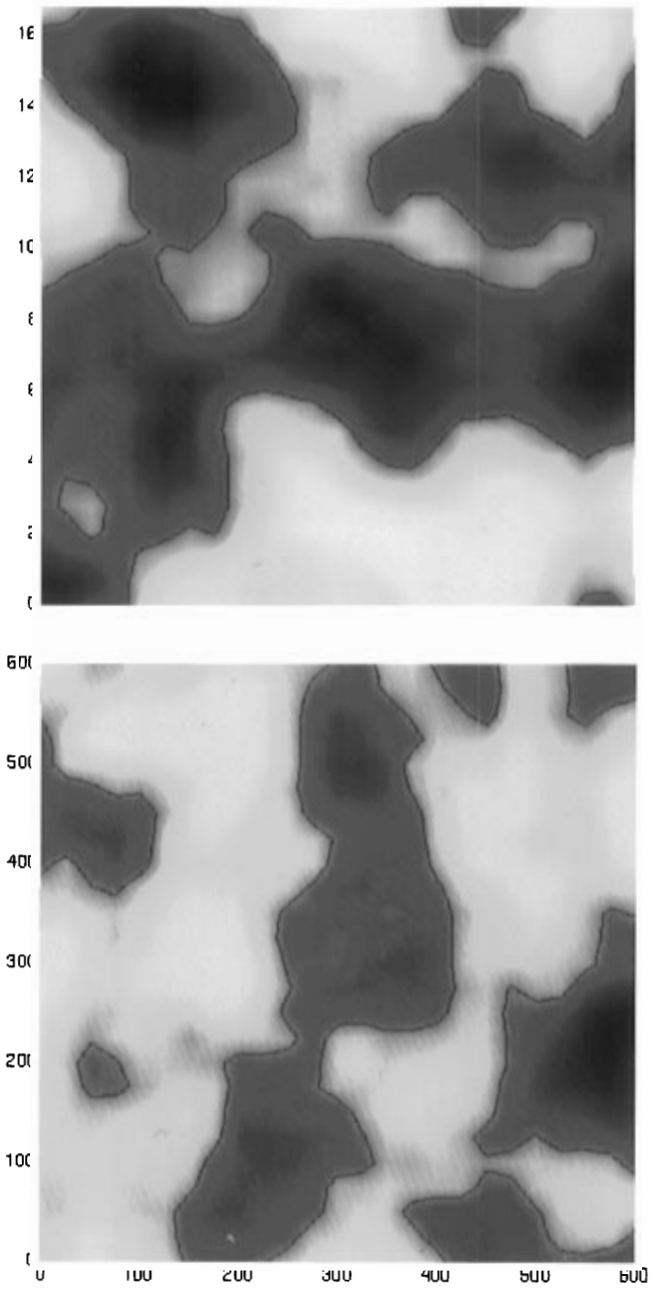

Figure 4. (a, top) Cross-sectional view of the 3D morphology generated by the MB theory for the dPB/PI blend ($16.8 \times 16.8\ \mu m^2$). (b, bottom) Cross-sectional view of the 3D morphology of the microemulsions (600×600 Å^2). The cross-sectioned views were obtained with infinitesimal thickness. The color graduations represent unclipped waves from eq 4, and the level set $\psi(\vec{r}) = 0$ is highlighted by black lines corresponding to the interface of the systems. The red and yellow regimes correspond to the two coexisting phases.

PI-rich phases for the polymer mixture or oil and water domains for the microemulsions, is drawn. Cross-sectional views of the two systems are also shown in Figure 4. These are the cross sections of the horizontal midplanes of the cubes shown in Figure 3. Although the characteristic lengths of the two systems were different by a factor of about 240, the morphologies appear quite similar to each other: the morphologies are bicontinuous and domains are interpenetrating. Although there are quantitative differences between the two structures, as revealed by the scattering profiles at low q values as well as the values of b/a, they are not visually self-evident. The differences are geometrically subtle and show up best in the scattering.

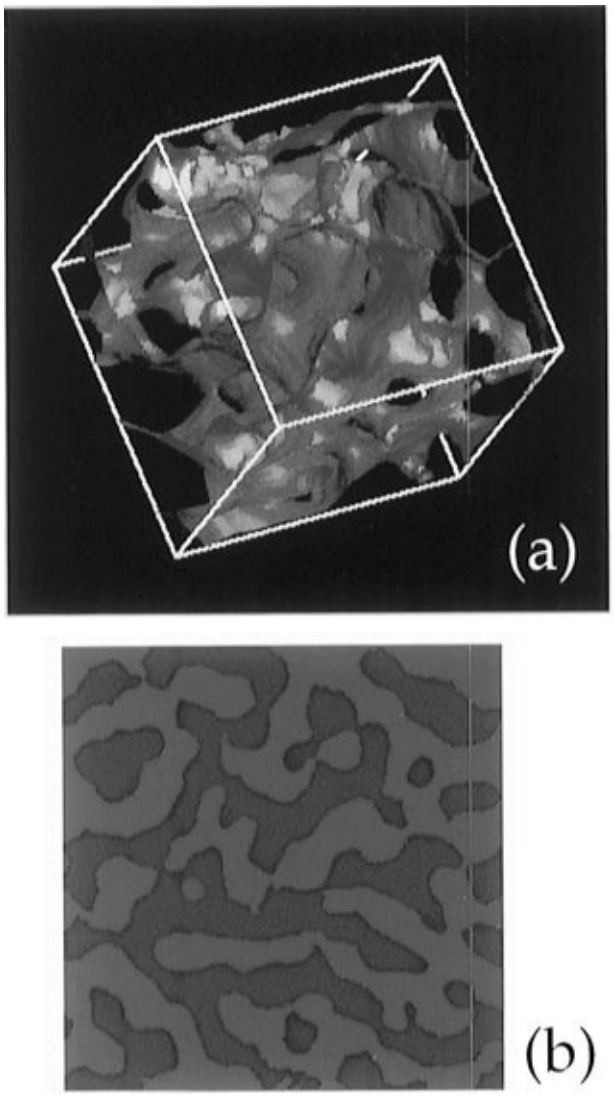

Figure 5. (a) 3D morphology of the SBR/PB blend (box size, 30^3 μm^3) showing the interfaces of two coexisting phases and (b) its cross-sectional view obtained by use of LSCM (cross-section size, 80×80 μm^2). The thickness of the optical slice was 0.65 μm.

Recently, it has been shown that a 3D real-space micrograph with a micrometer resolution can be obtained with the use of LSCM.[25] In Figure 5, a 3D image of the phase-separated structure (part a), as well as its cross-sectional view (part b), of a poly(styrene-*ran*-butadiene) (SBR)/poly(butadiene) (PB) blend developed via SD is shown. The method for obtaining the 3D image was described elsewhere.[25,26] It is worth noting that the structure factor obtained from the 3D LSCM image by a 3D Fourier transformation agreed with the measured LS scattering intensity profile of the dPB/PB blend and with the results of a computer simulation.[25] Thus, in a statistical sense, the 3D image presented in Figure 5 has essentially the same structure as the dPB/PI blend studied here. Similarity between the 3D morphologies generated by use of the MB theory for the dPB/PI blend and experimentally obtained from LSCM is reassuring.

On the basis of the MB theory, one can discuss curvature of the interface. The quantities to be investigated are the mean curvature, H, and the Gaussian curvature, K, which are respectively defined as an average and a product of two principal curvatures of the surface at the point of interest. From the three parameters obtained from the fit of the MB theory to the scattering intensity distribution, it is possible to estimate $\langle K \rangle$ of the internal interface by use of eq 13. Here, $\langle K \rangle = \int K(\vec{r})\, d\Sigma/\Sigma$ denotes the average of the local curvature at a position $\vec{r}$ on the surface over the whole connected surface Σ. The following argument is based on the assumption that the structure is isometric and H is zero. Jinnai et al. demonstrated from the direct analysis of the 3D LSCM image that the phase-separated structure of the SBR/PB polymer mixture had nearly zero mean curvature and negative $\langle K \rangle$.[27] Lee and Chen also concluded that $\langle H \rangle$ is effectively zero for the microemulsion by a SANS contrast variation method.[28] Moreover, Chen et al. concluded that $\langle K \rangle$ for the microemulsion was also negative.[13] Using eq 13 in conjunction with the three fitted parameters, we estimated $\langle K \rangle$. The values so obtained were -0.194 μm^{-2} for the polymer blend and -1.14×10^{-4} Å^{-2} for the microemulsion at 22 °C. It is important to note here that $\langle K \rangle$ is negative for both systems, suggesting that the interface of the polymer blend as well as the microemulsion is an anticlastic or saddle-like local feature almost everywhere.

Acknowledgment. We thank Mr. Kohtaro Kimishima for his assistance with the SAXS measurements. S.H.C. is grateful for the JSPS fellowship which made his stay at Kyoto University possible. Research of S.H.C. is supported by a grant from the U.S. DOE.

References and Notes

(1) Gunton, J. D.; San Miguel, M.; Sahni, P. In *Phase Transitions and Critical Phenomena*; Domb, C., Lebowitz, J. L., Eds.; Academic Press: New York, 1983; p 269.
(2) Hashimoto, T. *Phase Transitions* **1988**, *12*, 47. *Materials Science and Technology, Vol 12, Structure and Properties of Polymers*, VCH: Weinheim, 1993.
(3) Snyder, H. L.; Meakin, P. *J. Chem. Phys.* **1983**, *79*, 5588.
(4) Jahn, W.; Strey, R. *J. Phys. Chem.* **1988**, *92*, 2294. Chen, S. H.; Chang, S. L.; Strey, R. *J. Chem. Phys.* **1990**, *93*, 1907.
(5) Hashimoto, T.; Takenaka, T.; Jinnai, H. *J. Appl. Crystallogr.* **1991**, *24*, 457. Takenaka, M.; Hashimoto, T. *J. Chem. Phys.* **1992**, *96*, 6177.
(6) Jinnai, H.; Hasegawa, H.; Hashimoto, T.; Han, C. C. *J. Chem. Phys.* **1994**, *99*, 8154. Jinnai, H.; Hasegawa, H.; Hashimoto, T.; Han, C. C. *J. Chem. Phys.* **1994**, *99*, 8154.
(7) Furukawa, H. *Phys. Rev. Lett.* **1979**, *43*, 136. Furukawa, H. *Phys. Rev. B* **1986**, *33*, 638.
(8) Koga, T.; Kawasaki, K. *Physica A* **1993**, *196*, 389. Koga, T.; Kawasaki, K.; Takenaka, M.; Hashimoto, T. *Physica A* **1993**, *198*, 473.
(9) Ohta, T.; Nozaki, H. In *Space−Time Organization in Macromolecular Fluids*; Tanaka, F., Doi, M., Ohta, T., Eds.; Springer: Berlin, 1989; p 51.
(10) Berk, N. F. *Phys. Rev. Lett.* **1987**, *58*, 2718.
(11) Cahn, J. W. *J. Chem. Phys.* **1965**, *42*, 93.
(12) Chen, S. H.; Lee, D. D.; Chang, S. L. *J. Mol. Struct.* **1993**, *296*, 259.
(13) Chen, S. H.; Lee, D. D.; Kimishima, K.; Jinnai, H.; Hashimoto, T. *Phys. Rev. E*, in press.
(14) Debye, P.; Anderson, H. R., Jr.; Brumberger, H. *J. Appl. Phys.* **1957**, *28*, 679.
(15) Teubner, M. *Europhys. Lett.* **1991**, *14*, 403.
(16) Teubner, M.; Strey, R. *J. Chem. Phys.* **1987**, *87*, 3195.
(17) Chen, S. H.; Chang, S. L.; Strey, R. *J. Appl. Crystallogr.* **1991**, *24*, 721.
(18) This assumption is probably justified for the polymer blend in the late stage of SD, but it is only approximately true for a bicontinuous microemulsion. For the latter, one may take $\Lambda \approx d$. More precisely, the spectral function we introduced contains three length scales, although there may be some relations among them in real systems.
(19) Scattering intensity in eq 14 should be expressed not only as a function of q but also as a function of time, t, for the polymer mixture; the phase separation of the system is a non-equilibrium process, and thus, a time-dependent process. Since, in the present study, the time evolution of the phase-

separated structure is not the central issue, and we discuss the scattering intensity at a fixed time for the polymer blend, we simply write the scattering only as a function of q.

(20) Hayashi, M.; Jinnai, H.; Hashimoto, T. Manuscript in preparation.

(21) Porod, G. *Koll. Z.* **1951**, *124*, 83. Porod, G. *Koll. Z.* **1952**, *125*, 51. Porod, G. *Koll. Z.* **1952**, *125*, 108.

(22) Furukawa, H. *J. Phys. Soc. Jpn.* **1989**, *58*, 216.

(23) Yeung, C. *Phys. Rev. Lett.* **1988**, *61*, 1135.

(24) Furukawa, H. *Adv. Phys.* **1985**, *34*, 703.

(25) Jinnai, H.; Nishikawa, Y.; Koga, T.; Hashimoto, T. *Macromolecules* **1995**, *28*, 4782.

(26) Jinnai, H.; Yoshida, H.; Kimishima, K.; Hirokawa, Y.; Funaki, Y.; Hashimoto, T. Submitted to Macromolecules.

(27) Jinnai, H.; Koga, T.; Nishikawa, Y.; Hashimoto, T.; Hyde, S. T. Submitted to *Phys. Rev. Lett.*

(28) Lee, D. D.; Chen, S. H. *Phys. Rev. Lett.* **1994**, *73*, 106.

MA960486X